Available online at www.sciencedirect.com
SCIENCE DIRECT
Polymer 47 (2006) 3681–3688
polymer
www.elsevier.com/locate/polymer

The DFT study on the electronic structures of polytitasilanes: Several new classes of narrow band gap polymers

Yunqiao Ding, Dacheng Feng *, Shengyu Feng, Jie Zhang, Ju Xie

Institute of Theoretical Chemistry, Shandong University, Jinan 250100, People's Republic of China

Received 3 January 2006; received in revised form 8 March 2006; accepted 10 March 2006

Abstract

The exploring theoretical investigation on Ti-substituted polysilane model, $(Si_5TiH_{12})_n$, $(Si_3TiH_8)_n$ and $(SiTiH_4)_n$, has been performed by using density functional theory (DFT). Ti substitutions have little effect on geometrical structures. The characteristic IR band of Ti substitutions is at 1710–1760 cm^{-1}. TDDFT calculations on excited states illuminate that electronic spectrum absorption of polytitasilanes locates at visible light area (400–750 nm). Periodic density functional theory (PDFT) calculation on polymers shows the gap of polytitasilanes is lower greatly than the parent polysilane. Compared with the same size polysilane, with an increase of the Ti/Si ratio, the band gap is lowed by 2.0 eV for $(Si_5TiH_{12})_n$, 2.1 eV for $(Si_3TiH_8)_n$ eV and 2.2 eV for $(SiTiH_4)_n$d, that is to say, the higher the doping level of Ti atom is, the lower the gap is. Ti's 3d orbital in LUCB of Ti substitutions plays a significant role in the decrease of band gap.

Keywords: PDFT polytitasilane; Ti substitutions

1. Introduction

Polysilane is a new kind of macromolecule with unique σ-conjugation delocalized along silicon skeletons. The σ-conjugation gives polysilane highly unusual properties, such as photosensitivity, photoconductivity, nonlinear optical properties et al. Thus, polysilane has attracted much attention because of their potential technological applications [1]. In the 1980s of last century, Takeda et al. have performed a series of theoretical studies on polysilanes with the semiempirical and the local-density-functional (LDF) methods [2–5]. The theoretical results showed that one dimension (1D) ideal chain polysilane has a directly-allowed-type band structure with a band gap of about 3–4 eV; so they are semiconductors with great energy gap. In recent years, the new synthesis technologies of polysilane have been reported extensively. For example, Obata et al. reported a novel synthetic method for a linear polysilane using a photochemical vapor deposition (photo-CVD) method of a small cyclic oligosilane [6]. End-graft polysilane have been synthesized by Furukawa [7], which promoted the study of single polymer science. Tsukuda et al. used high-energy ion beams to fabricate the cross-linked polymer nanowires with a variety of Si-based polymers [8]. Along with development of novel polysilane used as functional materials, the theoretical calculation and simulation on electronic structures and optical characteristics of polysilane become hot topics [9–11].

In recent years, there have been tremendous research interests in the design and synthesis of narrow band gap (E_g) electroactive polymers because of their particular optoelectronic properties [12]. The magnitude of energy gap relates significantly to photoelectrical characteristics of polymer. Although polysilane is a sort of semiconductor polymer with a broad energy gap, there are many approaches for reducing the gap of polysilane and improving their photoelectrical characteristics. Modifying the side group or doping heteroatom or groups in backbone is familiar method for tailoring polysilane. Ti, which is a kind of nontoxic transition metal with the light atomic mass, has an electronic configuration of s^2d^2, which is similar to that of Si in a way. Furthermore, the analog of silane, TiH_4, has been identified experimentally [13]. Considering the noticeable feature of Ti element, we design a series of compounds in which Si atom of polysilane substituted by Ti partly in order to change the electron structure of polysilane. Our work interests in the differences of electronic structure between parent polysilane and Ti-substituted polysilanes that Ti atoms are introduced into silicon backbone of polysilane.

* Corresponding author. Tel.: +86 531 88365748; fax: +86 531 88564464.
E-mail address: fdc@sdu.edu.cn (D. Feng).

0032-3861/$ - see front matter © 2006 Elsevier Ltd. All rights reserved.
doi:10.1016/j.polymer.2006.03.042

In this paper, oligosilane and a series of oligomer models of Ti substitutions with different Ti/Si ratio have been studied by density functional theory (DFT). On the base of geometry optimized structure, we carried out the detailed analysis of electronic structure of oligosilanes and oligotitasilane. Besides, the electron band structure of 1D polysilane and polytitasilane ($(Si_{10}Ti_2H_{24})_n$, $(Si_6Ti_2H_{26})_n$ and $(Si_2Ti_2H_8)_n$) were calculated by periodic density functional theory (PDFT).

2. Computational model and method

The structures of ground-state dodecasilanes ($Si_{12}H_{26}$) and the same size Ti substitutions ($Si_{10}Ti_2H_{26}$, $Si_9Ti_3H_{26}$, $Si_6Ti_6H_{26}$) were optimized by Becke's three-parameter hybrid functional for exchange combined with the correlation functional due to Lee, Yang, and Parr (B3LYP) [14,15] at the 6-31G(d) levels. For comparison, all oligomer models were optimized using pure DFT method—BLYP [16,17] and density fitting basis sets 6-31G(d). The calculated models adopt transconfiguration, as shown by Fig. 1. Based on the optimized geometries at B3LYP/6-31G(d) levels, vibrational frequencies were computed in order to foresee infrared spectrum characteristics of Ti substitutions. Time-dependent DFT (TDDFT) [18–20] calculation on vertical excitation energies were performed. The calculations of nature bond orbital (NBO) [21–23] have been done for illuminating their bonding states.

The periodic boundary conditions (PBC) [18,24–26] calculations on one-dimensional (1D) polymer systems were carried out. Polymers are constituted by repeated monomers. For each polymer, (SiH_2), (Si_5TiH_{12}), (Si_3TiH_8) and ($SiTiH_4$) were defined as primitive unit cell, respectively. The repeated unit cells were combined into the larger 'supercell' which is twice as big as the primitive unit cells. The lengths of translation vectors (**a**) are 7.95 Å for (Si_2H_4), 24.20 Å for ($Si_{10}Ti_2H_{24}$), 16.22 Å for ($Si_6Ti_2H_{24}$) and 8.47 Å for ($Si_2Ti_2H_8$), respectively, see Fig. 2. It was found that convergence criteria was difficult to come to by using hybrid functional B3LYP on PBC calculations, considering calculating capability and practical efficiency, geometry optimization of polymers was carried out using BLYP method and density fitting basis sets 6-31G(d), and then the band structure calculations were performed and 20 *k*-points were calculated within the Brillouin zone. All calculations were performed using a Gaussian 03 program package [27].

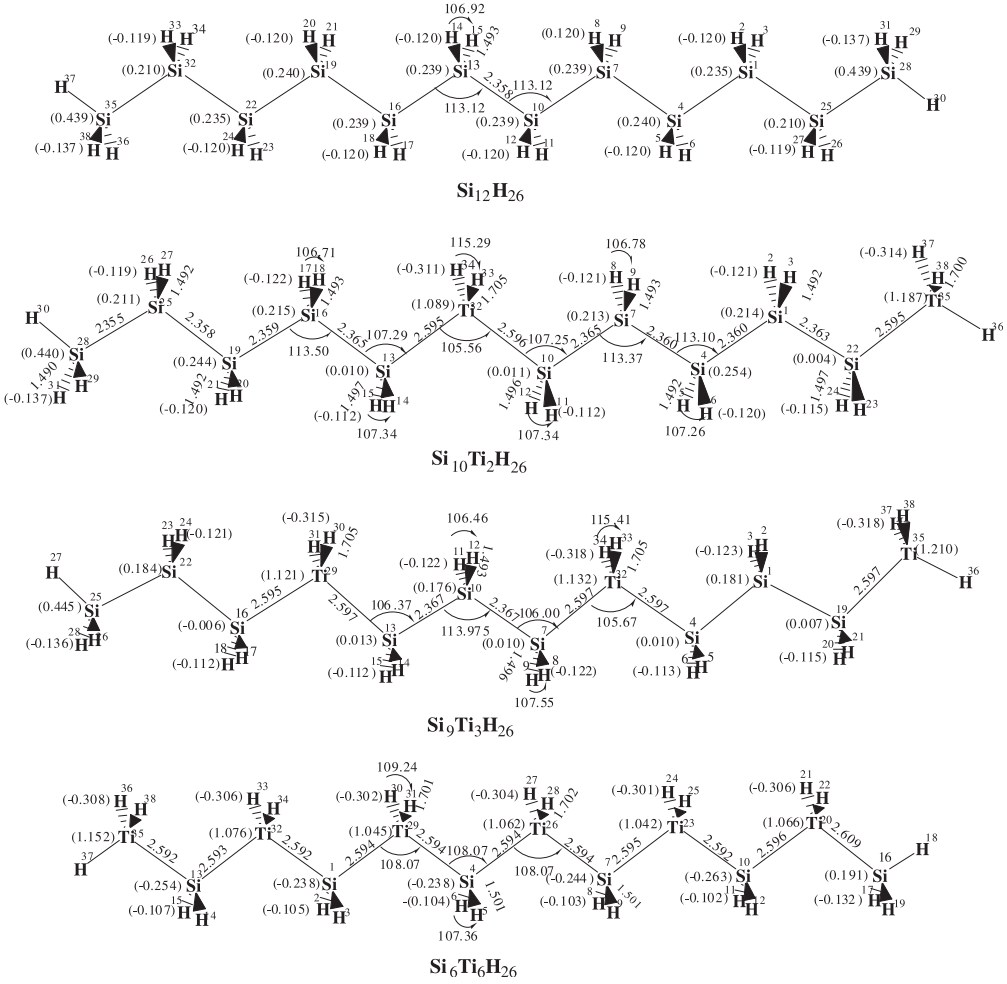

Fig. 1. Optimized geometry at the B3LYP/6-31G(d) of $Si_{12}H_{26}$ and oligotitasilane ($Si_{10}Ti_2H_{26}$, $Si_9Ti_3H_{26}$, $Si_6Ti_6H_{26}$) and their natural charge of atoms using NBO analyse at B3LYP/6-311++G(d,p)levels. Bond lengths are listed in angstrom and bond angles are in degrees. Arabic numerals are element labels.

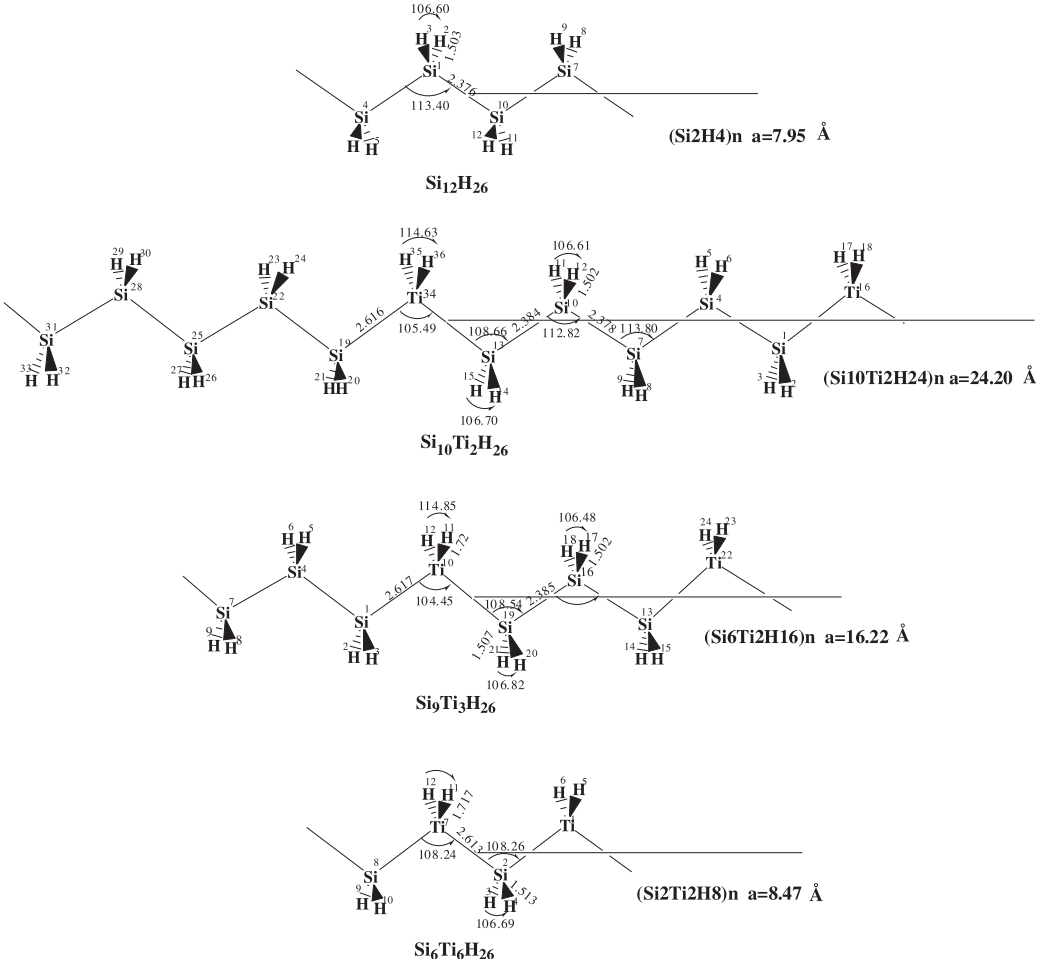

Fig. 2. Optimized unit cell geometrical structures of Si_nH_{2n+2} and $Si_{n-1}TiH_{2n+2}$ using periodic boundary condition (PBC) DFT theory. The letter *a* denote length of translation vectors and its unit of value is angstrom.

3. Results and discussion

3.1. Oligomer

3.1.1. Geometry structure

Fig. 1 shows the optimized geometry structural parameters of the dodecasilane ($Si_{12}H_{26}$) and the same size oligotitasilanes with different Ti/Si ratio ($Si_{10}Ti_2H_{26}$, $Si_9Ti_3H_{26}$, $Si_6Ti_6H_{26}$) at B3LYP/6-31G (d) levels and their natural charges (the numbers within brackets) at B3LYP/6-311 + + G (d, p). For comparison with B3LYP calculation, BLYP calculation was used to optimize all oligomers at the same basis sets, and compared results listed in Table 1.

The skeleton of dodecasilane is coplanar under B3LYP calculation. The Si–Si bond distance is about 2.36 Å optimized by B3LYP method and Si–H bond distance is about 1.49 Å at the same method. The silicon skeleton bear positive charges and the hydrogen atoms carry negative charges because the electronegativity of hydrogen is more than that of silicon.

A series of amorphous thin films of $Si_{1-x}Ti_x$ ($0<x<0.6$) [28], about 1 μm thick, has been made. Their structure measurements using extended X-ray absorption fine structure (EXAFS) and small-angle X-ray scattering (SAXS) showed that Si–Si bond length rise slowly from 2.34 to 2.38 Å with x increasing and Si–Ti bond with a range of 2.64 ± 0.03 Å is covalent.

As shown in Table 1, the optimized Si–Ti bond distance of oligotitasilanes is about 2.60 Å at B3LYP/6-31G (d) levels and shorter by 0.04 Å than that of $Si_{1-x}Ti_x$ ($0<x<0.6$) system mentioned above. Ti–H bond distance of $Si_{10}Ti_2H_{26}$ and $Si_9Ti_3H_{26}$ is about 1.70 Å at the same levels and this value is in good agreement with the experimental value (1.70 Å) of TiH_4 [13]. Results imply that both Si–Ti and Ti–H bond exist stably in oligotitasilanes. From $Si_{10}Ti_2H_{26}$ to $Si_9Ti_3H_{26}$, the Si–Si bond distances lengthen slightly from 2.37 to 2.38 Å with Ti atom increasing, which is in accordance with the tendency represented in the amorphous thin films of $Si_{1-x}Ti_x$. Both Si–Si bond length and Si–H bond length neighboring to Ti atom are longer only about 0.005 Å than the same bonds no neighboring to Ti atom. The bond angles of ∠ SiSiSi of Ti substitutions are slightly larger than those of dodecasilane. The dihedral angle ∠ SiSiSiSi of $Si_{10}Ti_2H_{26}$ and $Si_9Ti_3H_{26}$ are deviated from 180° slightly. The skeleton of $Si_6Ti_6H_{26}$ is nearly coplanar.

Table 1
The comparison of structure parameters optimized by B3LYP and BLYP at 6-31G(d) level

	$Si_{12}H_{26}$		$Si_{10}Ti_2H_{26}$		$Si_9Ti_3H_{26}$		$Si_6Ti_6H_{26}$	
	B3LYP	BLYP	B3LYP	BLYP	B3LYP	BLYP	B3LYP	BLYP
R_{Si-Si}	2.358	2.375	2.360	2.377				
R^*_{Si-Si}			2.365	2.383	2.367	2.385		
R_{Si-H}	1.493	1.502	1.497	1.502	1.493	1.502		
R^*_{Si-H}			1.493	1.508	1.496	1.507	1.501	1.501
R_{Si-Ti}			2.596	2.615	2.597	2.615	2.594	2.594
R_{Ti-H}			1.705	1.720	1.705	1.720	1.702	1.702
$A_{Si-Si-Si}$	113.12	113.40	113.37	113.24	113.98	113.50		
$A_{Si-Ti-Si}$			105.56	106.46	105.67	105.98	108.69	108.02
$D_{Si-Si-Si-Si}$	180.00	178.70	−179.08	−179.52				
$D_{Si-Si-Ti-Si}$			−175.13	−176.99	178.28	−174.13		
$D_{Si-Ti-Si-Si}$							−179.42	180

R* denotes bond parameter neighboring Si–Ti bond.

Table 2
The natural bond orbital occupancies of Si–Ti bond Si–Si and Si–H bonds at the B3LYP/6-311++g(d,p) levels

$Si_{12}H_{26}$	Occup.	$Si_6Ti_6H_{26}$	Occup.	$Si_9Ti_3H_{26}$	Occup.	$Si_{10}Ti_2H_{26}$	Occup.
BD ^{10}Si–^{13}Si	1.963	BD ^{4}Si–^{26}Ti	1.903	BD Si–^{32}Ti	1.945	BD ^{10}Si–^{32}Ti	1.953
BD ^{10}Si–^{11}H	1.985	BD ^{4}Si–^{5}H	1.964	BD ^{7}Si–^{10}Si	1.934	BD ^{0}Si–^{11}H	1.977
				BD ^{7}Si–^{8}H	1.977	BD ^{4}Si–^{7}Si	1.955
				BD ^{0}Si–^{11}H	1.984	BD ^{4}Si–^{5}H	1.985

NBO calculations show that in oligotitasilanes, Ti atoms bear negative charges and the Si atoms bonded with Ti bear positive charges (Table 2). In particular, the atoms charges of backbone of $Si_6Ti_6H_{26}$ take on the alternate distribution between negative and positive. The natural bond orbital occupancies and corresponding NAO bond order of Si–Si/Si–H in oligotitasilanes are a little lower than that of Si–Si/Si–H in oligosilane, so the bond strength of the backbone is not obviously weakened by Ti substitution (Tables 2 and 3). As mentioned above, Ti substitutions might be a sort of stable compounds.

3.1.2. Frontier molecular orbitals analysis

In order to understand Ti substitutions systems well, it is essential to investigate their electronic structures. Although DFT method cannot describe accurately the HOMO–LUMO gap, the 'band gap' (E_g), the difference between the highest occupied molecular orbital (HOMO) energy and the lowest unoccupied molecular orbital (LUMO) energy, can be estimated by DFT calculation. Constitution and characteristics of the frontier molecular orbitals of oligosilane and oligotitasilanes were also discussed using DFT method. Orbital contours are described in Fig. 3.

The HOMO (MO=97) of the dodecasilane is mainly composed of the σ-bonding orbital between two Si's $3p_x$ orbital along the skeleton axial direction LUMO (MO=98) is mainly composed of the σ*-antibonding orbitals between two Si's $3p_y$ orbital. In occupied orbital, there are many big σ bond orbital spreading over several atoms in backbone (such as, MO=93, 95).

The HOMO of the same size Ti substitutions is similar to that of dodecasilane, except that the titanium's 3d orbital contributed to bonding in the former skeleton. The HOMO of oligotitasilanes are mainly composed of the σ-bonding state between Si's 3p orbital and Ti's 3d orbital and σ-bonding state between Si's 3p orbitals mixing Si's 3s orbitals along the skeleton axial direction. LUMO of oligotitasilanes are all derived from Ti's 3d orbitals mixing with Si's 3s orbitals.

3.1.3. IR analysis

In order to compare the infrared spectrum (IR) characteristics between oligosilane and oligotitasilanes, the IR were simulated at the B3LYP/6-31G(d) levels. A set of IR value of butasilane (Si_4H_{10}) were calculated firstly at the same levels for testifying the reliability of the calculations, the small differences between calculated and experimental values

Table 3
Calculated atom–atom overlap-weighted NAO bond order at the B3LYP/6-311++g(d,p) levels

$Si_{12}H_{26}$	Bond order	$Si_6Ti_6H_{26}$	Bond order	$Si_9Ti_3H_{26}$	Bond order	$Si_{10}Ti_2H_{26}$	Bond order
^{10}Si–^{13}Si	0.827	^{4}Si–^{26}Ti	0.638	^{13}Si–^{29}Ti	0.626	^{10}Si–^{32}Ti	0.629
^{10}Si–^{11}H	0.773	^{4}Si–^{5}H	0.760	^{13}Si–^{10}Si	0.815	^{7}Si–^{10}Si	0.817
				^{13}Si–^{14}H	0.771	^{4}Si–^{7}Si	0.823
				^{10}Si–^{11}H	0.772	^{10}Si–^{11}H	0.771
						^{7}Si–^{8}H	0.771

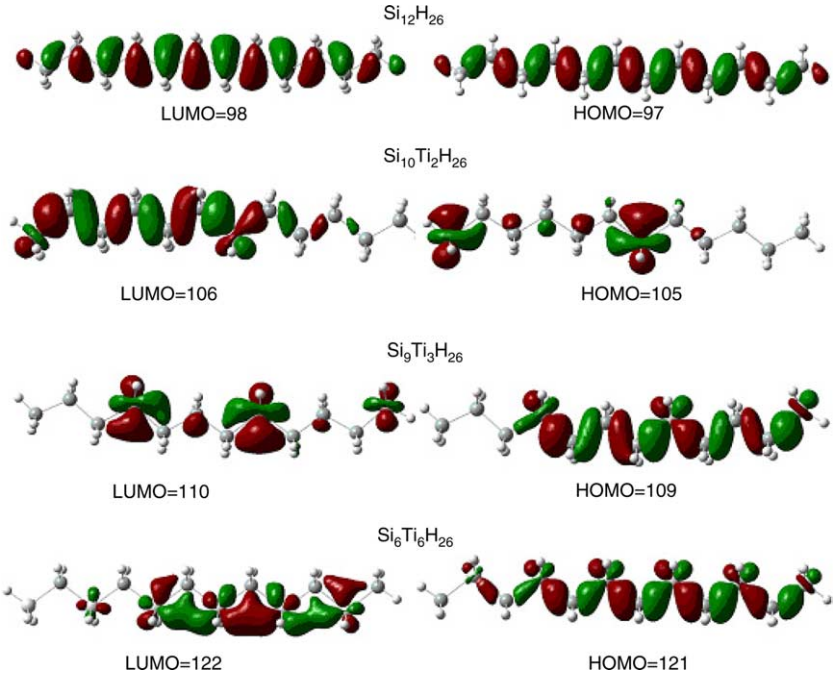

Fig. 3. Frontier molecular orbitals contours.

indicate that the calculations at B3LYP/6-31G(d) levels are reliable (Table 4).

Characteristic infrared absorption of oligosilanes ($Si_{12}H_{26}$) has four spectrum bands: 582 cm^{-1} (the wagging vibration of SiH_2, ω_{SiH_2}); 890 cm^{-1} (the wagging vibration of ended SiH_3 group, ω_{SiH_3}); 943–953 cm^{-1} (the scissor vibration of SiH_2, δ_{sSiH_2}); 2210–2250 cm^{-1} (symmetric stretch vibration of SiH_3 and asymmetrical stretch vibration of SiH_2, ν_{sSiH_2} and ν_{asSiH_2}). The first band is a single sharp peak with strong intensity. Other three bands are all broad absorptions consisted of multiple peaks. The infrared absorption intensity of Si–Si bond is very weak and approximately equal to zero.

Characteristic bands for oligotitasilanes are at 1710–1760 cm^{-1}, and with increasing of Ti/Si ratio, the intensity of band strengthen little by little. They are assigned to symmetric stretch vibration of TiH_2 (ν_{sTiH_2}), and asymmetrical stretch vibration of the TiH_3 (ν_{asTiH_3}), respectively. The infrared absorption intensity of Si–Ti bond is also very weak, and the location is 301 cm^{-1} for $Si_6Ti_6H_{26}$ and 309 cm^{-1} for $Si_9Ti_3H_{26}$ and 312 cm^{-1} for $Si_6Ti_6H_{26}$. For $Si_6Ti_6H_{26}$ the strong band around 361 cm^{-1} is assigned to the wagging vibration of TiH_2 (ωTiH_2), however, it is not existed in other Ti substitutions. Compared to ωSiH_2 of $Si_{12}H_{26}$, ωSiH_2 of $Si_{10}Ti_2H_{26}$ was blue shift by 32 cm^{-1}, and ωSiH_2 of $Si_9Ti_3H_{26}$ was blue shift by 47 cm^{-1}, however, the intensity of ωSiH_2 for $Si_6Ti_6H_{26}$ is weak. The band at 2210–2250 cm^{-1} of oligosilane were also found in oligotitasilanes, and corresponding intensity decreases greatly with increasing of Ti/Si ratio. Compared to ν_{asSiH_2} of $Si_{12}H_{26}$, that of $Si_6Ti_6H_{26}$ were blue shift by 57 cm^{-1}, but for $Si_9Ti_3H_{26}$ and $Si_{10}Ti_2H_{26}$, the band of ν_{asSiH_2} increases no more.

3.1.4. Energy level and electronic spectrum analysis

It is well known that strong electronic absorption in the near UV region (200–400 nm) is remarkable spectrum nature of polysilane compounds. Energy level analysis and single excited state energy were carried out for estimating and forecasting qualitatively electronic excited state properties of present systems (Fig. 4).

Fig. 5 shows calculated electron-energy levels of $Si_{12}H_{26}$, $Si_{10}Ti_2H_{26}$, $Si_9Ti_3H_{26}$ and $Si_6Ti_6H_{26}$ at B3LYP/6-311++G(d,p) levels. The HOMO–LUMO gap difference between dodecasilane and Ti-substituted dodecasilanes is 1.94 eV for $Si_{10}Ti_2H_{26}$ and $Si_{12}H_{26}$, 2.18 eV for $Si_9Ti_3H_{26}$ and $Si_{12}H_{26}$, 2.58 eV for $Si_6Ti_6H_{26}$ and $Si_{12}H_{26}$, respectively. HOMO–LUMO gap of Ti-substitution was lowered greatly due to the hoist of the HOMO level and the great fall of LUMO level. It implies that their maximum UV absorption may be red shift compared to the same size polysilane. For Ti-substituted systems, with the increases of Ti/Si ratio, the gap decreased. The analysis of frontier molecular orbital has explained that the Ti' 3d orbital of the LUMO in oligotitasilanes leads to decreasing in the energy of LUMO, further, reducing the gap.

Table 4
The comparison of vibrational spectrum of Si_4H_{10} between calculated values and the experimental values [16]. Experimental data obtained from [29].

Model	B3LYP/6-31G(d)		
	$F_{cal.}$ (cm^{-1})	F_{Exp} (cm^{-1})	$\Delta_{Exp-cal}$
ωSiH_2	680	692	12
ωSiH_3	885	874	11
$\delta_s SiH_2$	955	933	22

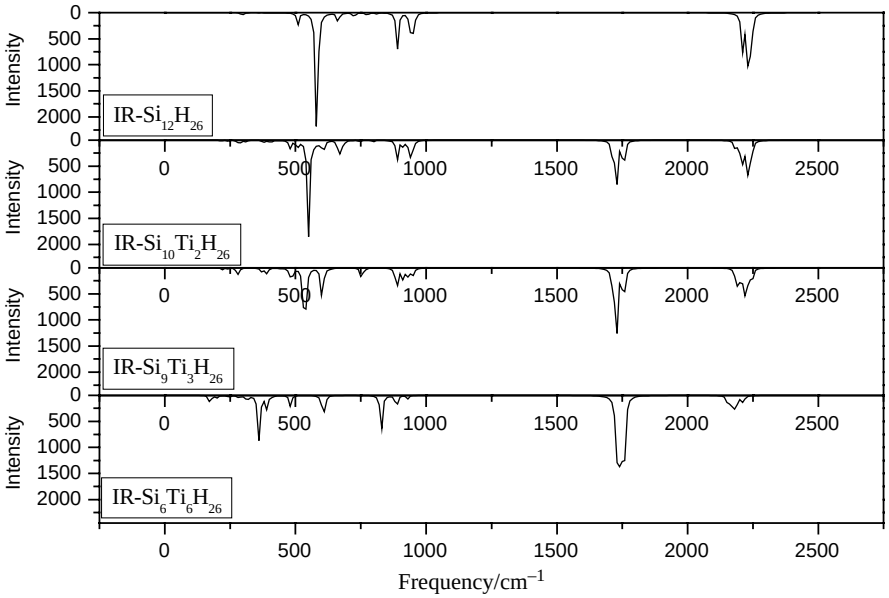

Fig. 4. The intimidated infrared spectrum of $Si_{12}H_{26}$, $Si_{10}Ti_2H_{26}$, $Si_9Ti_3H_{26}$ and $Si_6Ti_6H_{26}$ at B3LYP/6-31G(d) levels.

Table 5 lists the calculated results of singlet excited state energy at B3LYP/6-3IG (d) levels. It can be found that the first singlet excited states (S_1) energy of Ti substitutions is greatly lower than that of dodecasilane, and maximum absorption of Ti substitutions enters into visible light area (380–780 nm). In present Ti substitutions, with increasing of Ti/Si ratio, the energy of S_1 lowers by 0.053 eV in turn.

3.2. Polymer

It is found that the convergence is difficult by using B3LYP method, so BLYP calculation at density fitting basis sets 6-3 1/G (d) level for the polysilane and polytitasilanes was performed using periodic boundary conditions. As shown in Table 1 the structural differences between B3LYP and BLYP is minimal, so the calculation of BLYP method is reliable.

Repeated unit constructs the polymers. The optimized configurations of polytitasilanes are similar to those of polysilanes, viewed by Fig. 2. In fact, the geometrical conformation of the polymer is the extension of monomer. With the exception of Si–Si/Si–H bond neighboring Si–Ti bond, Si–Si/Si–H bond length of polytitasilanes is about 2.38 Å/1.50 Å and is not longer than that of polysilane. The Si–Ti bond length is about 2.62 Å for $(Si_5TiH_{12})_n$ and $(Si_3TiH_8)_n$, and 2.61 Å for $(SiTiH_4)_n$. For polymer, Ti substitution exerts little influence on molecular conformation.

The analysis of the energy band structures will give very useful information of the optical and electrical properties of the polymers. Based on optimized structure, the polymers' energy band structures were calculated and diagrammed in Fig. 6(a)–(d). The *x*-axis represents the *K*-points within the Brillouin zone and the *y*-axis is the values of energy for each *K* points. The orbital contour plots for HOMO and LUMO were plotted on the right of Fig. 6.

The PBC band calculation of polysilane results in a directly-allowed-type band structure with a band gap of 3.47 eV. Fig. 6(a) shows that the calculated band gap of model polysilane is lower 0.28 eV than experimental one (3.76) [10]. The maximum direct gap is 6.77 eV The top of the valence band (HOVB) and the bottom of the conductor band (LUCB) are all located $k=0$. The HOVB comes from the σ-bonding orbital of Si's Si-3p_x along the skeleton. The LUCB is formed by the σ*-antibonding orbital of Si's 3sp_z orbital mixing with H's 1s orbital. Except for p σ bonds and antibonds, we also found big σ bond spreading over several atoms along backbone for example, MO=31 and pseudo-π bonds (MO= 29,30,34,35,37).

For $(Si_5TiH_{12})_n$ the minimal direct gap is 1.48 eV, and the maximal direct gap is 1.57 eV. The HOVB state is composed of two parts, the one is derived from the σ bonding state between

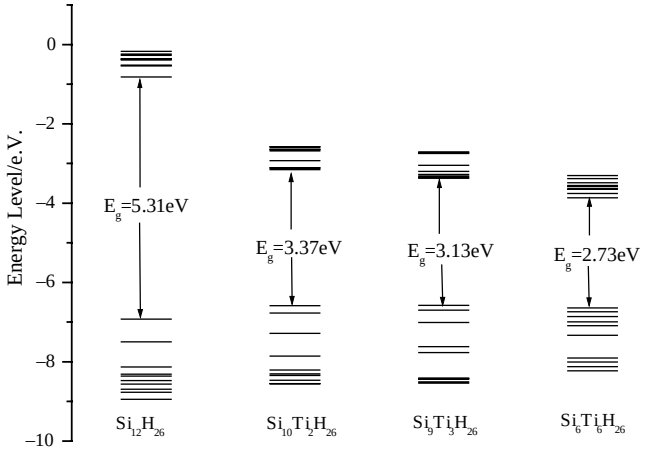

Fig. 5. Calculated electron-energy levels for dodecasilane and oligotitasilane models with optimized geometry using the DFT method at B3LYP/6-311++G(d,p) levels.

Table 5
The partial calculated results of S_1 excited state energy calculation using the time-dependent B3LYP/6-31G (d) method

	$Si_{12}H_{26}$	$Si_{10}Ti_2H_{26}$	$Si_9Ti_3H_{26}$	$Si_6Ti_6H_{26}$
E (eV)	4.82	1.80	1.75	1.70
$\lambda_{max/single}$ (nm)	257.18	686.22	706.94	728.75

Si's $3p_x$ orbital mixing with Si's 3s and Ti-$3d_{xy}$ orbitals, the other is the σ bonding orbital between the two Si's $3p_x$ orbitals. The LUCB state is Ti's $3d_{x^2-y^2}$ orbitals. In VB σ bond spreads only over a range of about four Si atoms (MO=97,99), and localized pseudo-π bond are buried in CB (MO=106,107,110,111).

For $(Si_3TiH_8)_n$, its band structure is very similar to $(Si_5TiH_{12})_n$. The minimal direct gap is 1.37 eV and the maximal direct gap is 1.55 eV. The matters of HOVB and LUCB is analogous to $(Si_5TiH_{10})_n$. In unoccupied orbitals, there are localized pseudo-π bonds (MO=78,79).

As shown in Fig. 5(d), PBC band structure calculation of $(SiTiH_4)_n$ results in the analogous 'direct-allowed-type' band structure with a minimal direct gap of 1.27 eV and maximal direct gap of 1.57 eV. Compared with $(Si_2H_4)_n$, the minimum gap reduced by 2.20 eV and maximal gap reduced by 5.20 eV; the energy of HOVB hardly change, but the energy of LUCB is only about half smaller than that of the polysialnes. The HOVB is constructed by the σ bonding orbital between Si-$3p_x$ and Ti-$3d_{xy}$ orbitals. The LUCB is mainly composed by Ti's $3d_{x^2-y^2}$ orbitals mixing with Si's orbital. There are pd pseudo-π bonds delocalized in CB.

Comparing the PBC energy band structure of polytitasilane models with that of polysilane, it can be found that the great differences between two polymers lies in CB's rather than in VB', that is, the energy of HOCO hardly change, but the energy of LOCO has been decreased greatly. It leads to the decrease of the energy gap of polytitasilane. The reason results from Ti' 3d orbital in LUCB of polytitasilanes, and yet LUCB of polysilane is σ*-antibond orbital. With the increasing of Ti/Si ratio, the gap of polytitasilanes decreases. The bandwidths of HOVB and LUCB of polytitasilanes become narrower than those of polysilane, and that the difference between minimal direct gap and the maximal direct gap become smaller greatly than that of polysilane. See Fig. 6(b)–(d), the two bands of HOVB and LUCB incline to parallel.

4. Conclusions

The structural and electronic properties of polysilane and its Ti substitutions were investigated by DFT method. Geometries of Ti substitutions are very similar to their parent polysilane. IR calculations foresee that characteristic IR spectrum band of Ti substitutions is at 1710–1760 cm^{-1}, and that the intensity of band strengthen is decreasing with increase of Ti/Si ration. TDDFT calculations imply that characteristic electron absorption of Ti substitutions take place obvious red shift compared to parent polysilane and enter into visible light area.

Periodic density function theory calculations on polymers showed that polytitasilanes have a directly allowed type band structure with a 1.48 eV gap for $(Si_5TiH_{12})_n$, 1.37 eV gap for $(Si_3TiH_8)_n$ and 1.27 eV gap for $(SiTiH_4)_n$. Due to Ti substitution, the band gap of polysilane is lowered greatly, and the higher Ti/Si ratio is, the lower gap is. The decreasing of gap contributes primarily to the LUCB's energy decreasing.

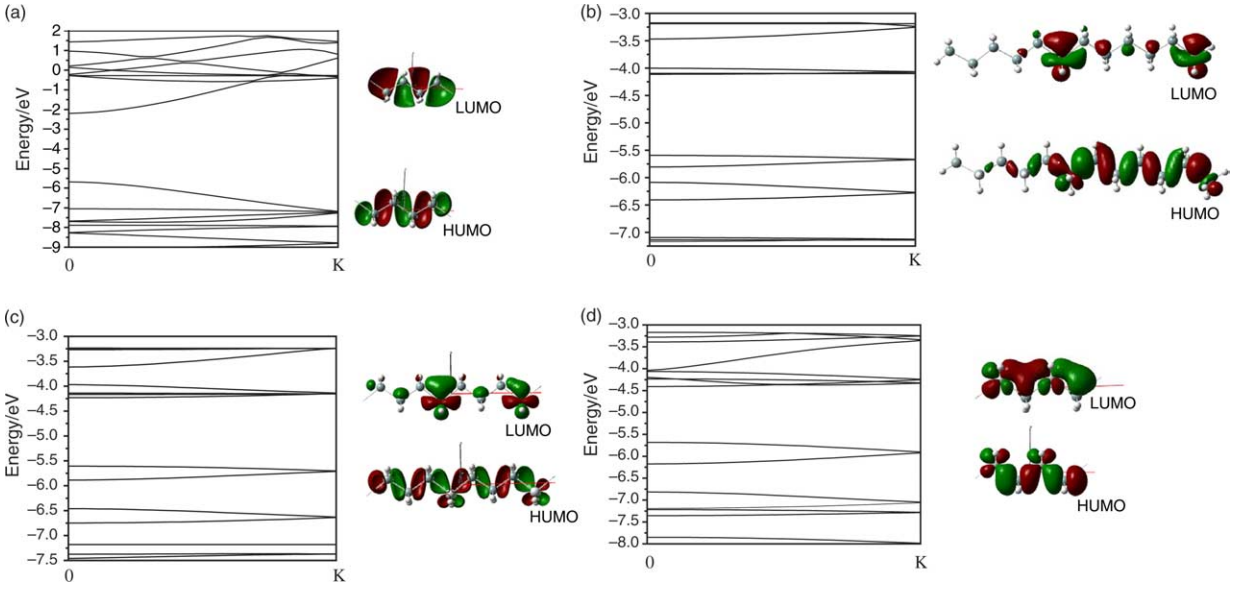

Fig. 6. (a) Electronic structure of the $(Si_2H_4)_n$ with a transplanar zigzag form. $E_{HOCO}=-5.66$ eV, $E_{LUCO}=-2.18$ eV. Max direct gap is 6.77 eV, min direct gap is 3.47 eV. Indirect gap is 3.47 eV. The orbital contour plots for HOMO and LUMO are shown on the right. (b) Electronic structure of the $(Si_5TiH_{12})_n$ copolymer with a transplanar zigzag form. $E_{HOCO}=-5.59$ eV, $E_{LUCO}=-4.11$ eV. Max direct gap is 1.57 eV, min direct gap is 1.483 eV. Indirect gap is 1.48 eV. The orbital contour plots for HOMO and LUMO are shown on the right. (c) Electronic structure of the $(Si_3TiH_8)_n$ copolymer with a transplanar zigzag form. $E_{HOCO}=-5.61$ eV, $E_{LUCO}=-4.23$ eV. Max direct gap is 1.55 eV, min direct gap is 1.37 eV. Indirect gap is 1.37 eV. The orbital contour plots for HOMO and LUMO are shown on the right. (d) Electronic structure of the $(SiTiH_2)_n$ alternating copolymer with a transplanar zigzag form. $E_{HOCO}=-5.68$ eV, $E_{LUCO}=-4.41$ eV. Max direct gap is 1.57 eV, min direct gap is 1.27 eV. Indirect gap is 1.27 eV. The orbital contour plots for HOMO and LUMO are shown on the right.

The formation of Ti' 3d orbital in LUCB of polytitasilanes plays an important role in decrease of band gap. Ti substitution might be a promising strategy to explore potential conducting polysilane.

Acknowledgements

This work was supported financially by the National Nature Science Foundation of China (No. 29974016), PhD Special Research Foundation of Chinese Education Department and the High Performance Computational Center of Shandong University.

References

[1] Cui X, Kertesz M. Macromolecules 1992;25:1103–8.
[2] Takeda K, Matsumoto N. Phys Rev B 1984;30:5871–6.
[3] Takeda K, Matsumoto N. J Phys C: Solid State Phys 1985;18:6121–33.
[4] Takeda K, Shiraishi K. Phys Rev B 1989;39:11028–37.
[5] Takeda K, Shiraishi K. J Am Chem Soc 1990;112:5043–52.
[6] Obata K, Sakamoto K, Kira M. Macromolecules 2001;34(9):2739–41.
[7] Furukawa K. Acc Chem Res 2003;36(2):102–10.
[8] Tsukuda S, Seki S, Tagawa S, Sugimoto M, Ldesaki A, Tanaka S, et al. J Phys Chem B 2004;108(11):3407–9.
[9] Ichikawa T, Kumagai J, Koizumi H. J Phys Chem B 1999;103(19): 3812–7.
[10] Sakurai Y, Yoshimura D, Ishii H, Ouchi Y, Isaka H, Teramae H, et al. J Phys Chem B 2001;105(24):5626–9.
[11] Elmaci NE. Yurtseves E. J Phys Chem A 2002; 106(49):11981–986.
[12] Lee Y, Sadki S, Tsuie B, Reyndds JR. Chem Mater 2001;13(7):2234–6.
[13] Hood DM, Pitzer RM, Schaefer III HF. J Chem Phys 1979;71:705.
[14] Becke AD. J Chem Phys 1993;98:5648.
[15] Becke AD. Phys Rev A 1988;38:3098.
[16] Lee C, Yang W, Parr RG. Phys Rev B 1988;37:785.
[17] Miehlich B, Savin A, Stoll H, Preuss H. Chem Phys Lett 1989;157:200.
[18] Zhang G, Ma J, Jiang Y. J Phys Chem B 2005;109:13499–509.
[19] Stratmann RE, Scuseria GE, Frisch MJ. J Chem Phys 1998;109:8218.
[20] Bauernschmitt R, Ahlrichs R. Chem Phys Lett 1996;256:454.
[21] Carpenter JE, Weinhold F. J Mol Struct (Theochem) 1988;169:41.
[22] Carpenter JE. PhD Thesis. Madison, WI: University of Wisconsin; 1987.
[23] Reed AE, Weinhold F. J Chem Phys 1983;78:4066.
[24] Kudin KN, Scuseria GE. Chem Phys Lett 1998;283:61.
[25] Kudin KN, Scuseria GE. Phys Rev B 2000;61:16440.
[26] Kudin KN, Scuseria GE. Phys Rev B 2002;65:205117.
[27] Frisch MJ, Trucks GW, Schlegel HB, Scuseria GE, Robb MA, Cheeseman JR, et al. Gaussian, Inc., Pittsburgh PA; 2003.
[28] Gurman SJ, Williams BT, Amiss JC. J Phys: Condens Matter 2000;12: 5981–90.